

Development of Bio-inspired Underwater Robot with Adaptive Morphology Capable of Multiple Swimming Modes

Thibaut Paschal, Jun Shintake, Stefano Mintchev and Dario Floreano

Abstract— Bio-inspired underwater robots have several benefits compared to traditional underwater vehicles such as agility, efficiency, and an environmentally friendly body. However, the bio-inspired underwater robots developed so far have a single swimming mode, which may limit their capability to perform different tasks. This paper presents a re-configurable bio-inspired underwater robot that changes morphology to enable multiple swimming modes: octopus-mode and fish-mode. The robot is 60 cm long and 50 cm wide, weighing 2.1 kg, and consists of a re-configurable body and 8 compliant arms that can be actuated independently. While the octopus-mode is expected to have unique abilities, question is if the fish-mode has distinctive advantages. With this platform, we investigate effectiveness of adaptive morphology in bio-inspired underwater robots. For this purpose, we evaluate the robot in terms of the cost of transport and the swimming efficiency of both the morphologies. The fish-mode exhibited a lower cost of transport of 2.2 and higher efficiency of 1.2 % compared to the octopus-mode, illustrating the effect of the multiple swimming modes by adaptive morphology.

I. INTRODUCTION

Recently, the scope of underwater robots expands to increasingly demanding applications such as environmental monitoring, marine ecosystems study, and inspection of submerged structures.

Bio inspiration is a promising design method for underwater robots given that bio-inspired locomotion can provide benefits not achievable by traditional marine propellers. Aquatic animals resulting of million years of evolution are endowed with a variety of morphological features for moving through water with high speed, agility and efficiency [1]. In addition, aquatic animals have environmentally friendly body. Thus, recent years have witnessed significant research work in the development of bio-inspired underwater robots in various swimming morphologies. These robots include fish and manta-ray that are driven by soft pneumatic actuators [2], [3], squid composed of multiple servo motors [4], magnetically driven eel [5], jellyfishes based on shape memory alloys or electroactive polymers [6], [7], and octopuses that have silicone based compliant arms moved by servomotors [8].

With the many underwater applications the world faces, it becomes required for underwater robots to have high capabilities and be multitasking. However, bio-inspired underwater robots developed up to now have a single

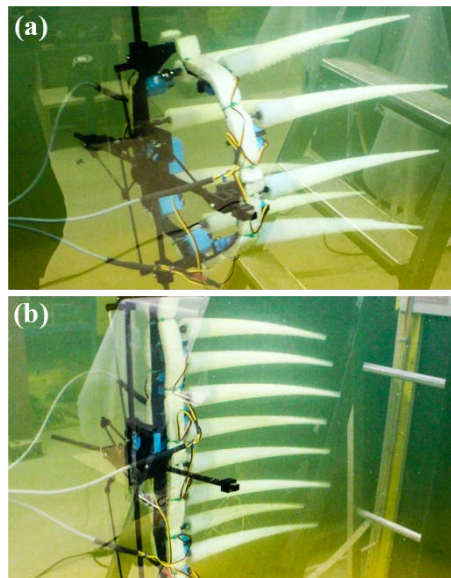


Fig. 1. The prototype of re-configurable underwater robot developed in this study. (a) The octopus morphology. (b) The fish morphology.

morphology resulting in the use of a specific swimming locomotion. This may limit their capability to deal with different tasks. For example, octopus-inspired robots are advantageous for activities at relatively low speed such as point observation, manipulating object and ground locomotion [9], but may not be suitable for traveling a long distance with high swimming speed and efficiency. Similarly, fish-inspired robots may have advantage on efficient, fast steady swimming, but their non-holonomic movement may have a difficulty when they are required to perform precise manoeuvring at low or zero forward speed. In this context, adaptation of morphology [10] to suitable swimming locomotion mode could be a solution to increase the range of manageable tasks.

This paper aims to investigate effectiveness of adaptive morphology in bio-inspired underwater robots. For this purpose, we propose a novel type of underwater robot combining fish-like swimming mode and octopus-like swimming mode as representative adaptive morphologies in a single platform. We demonstrate a proof of concept through the development of a prototype that has 8 compliant arms and a re-configurable body which can change its morphology to the octopus-mode (Fig. 1(a)) and the fish-mode (Fig. 1(b)). While the octopus-mode is expected to perform unique tasks such as object manipulation and ground locomotion as demonstrated in literature [9], question is if the robot in the fish-mode has unique advantages, for example, to swim faster and efficiently to travel long distance. Therefore, with this

This work was supported by the Swiss National Centre of Competence in Research (NCCR) Robotics.

T. Paschal, J. Shintake, S. Mintchev and D. Floreano are with the Laboratory of Intelligent Systems (LIS), Ecole Polytechnique Fédérale de Lausanne, Route Cantonale, Lausanne 1015, Switzerland (e-mail: {thibaut.paschal, jun.shintake, stefano.mintchev, dario.floreano}@epfl.ch).

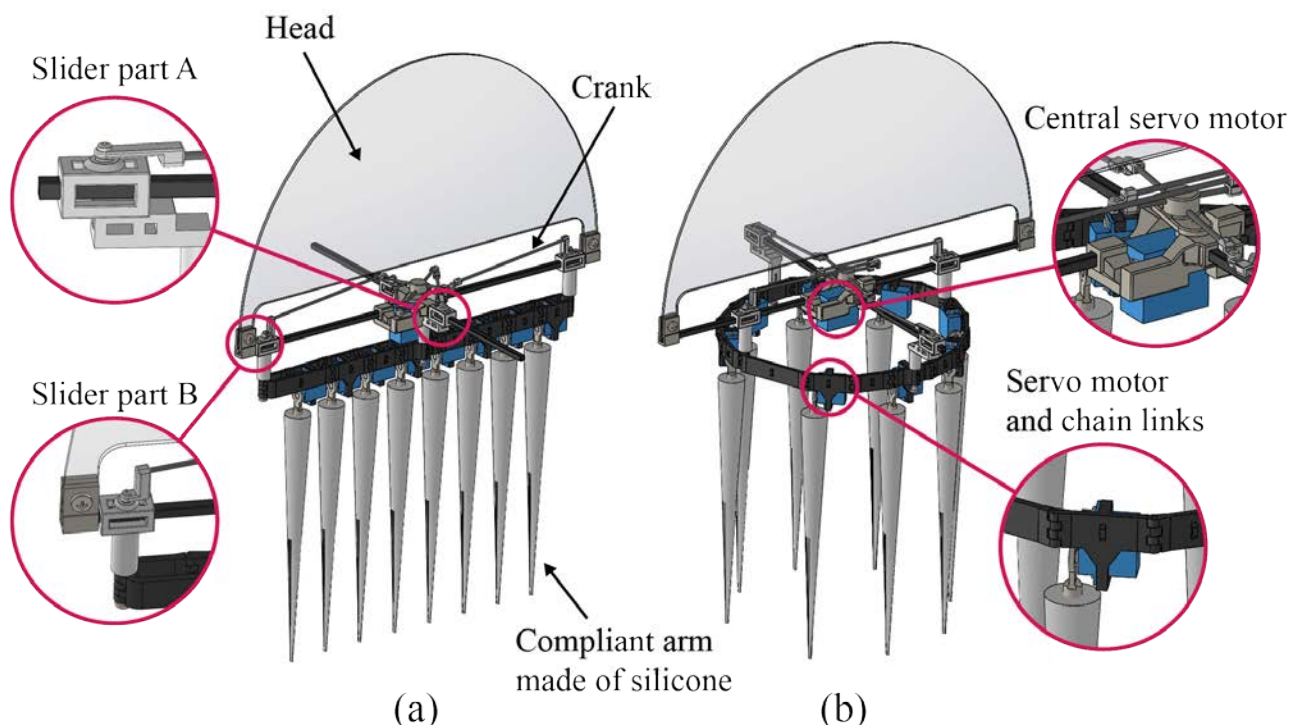


Fig. 2. Schematics of the underwater robot in (a) the fish morphology and (b) the octopus morphology.

platform, we evaluate the cost of transport and the swimming efficiency of both the morphologies. To obtain these performance characteristics, we measure the swimming speed, power consumption, and thrust force of the robot in both configurations during forward swimming.

In the rest of the paper, the robot's concept and mechanism are explained in Section II. The fabrication of the prototype is presented in Section III. The characterization of the prototype is performed in Section IV, followed by the discussion in Section V.

II. CONCEPT AND MECHANISM

The underwater robot consists of a re-configurable body and 8 compliant arms that can be actuated independently by 8 servomotors. Fig. 2(a) and (b) show the robot in the fish-mode and the octopus-mode, respectively. The reconfigurable body is composed of chain links that are connected to cranks, sliders, and the central servomotor. On the chain links, the compliant arms (therefore the servomotors) are placed with equal spacing. Once the central servo is actuated, the re-configurable mechanism allows the chains to change the shape between a straight (fish-mode) and a circle (octopus-mode), resulting in the modification of the robot morphology.

In the two morphologies, thrust force pushing the robot forward is generated by oscillating each compliant arm simultaneously. Even though we focus on the forward swimming in this paper, both the morphologies essentially have ability to achieve turning motion like roll, pitch and yaw, by changing the input for the servomotors such as the amplitude, offset, and frequency. As demonstrated in



Fig. 3. Silicone based compliant arm and mold.

literature, the octopus-mode also allows the robot to do object manipulation and walking on the ground [9].

III. FABRICATION OF PROTOTYPE

In order to prove the concept, we designed and fabricated a prototype. The compliant arms were fabricated using a soft silicone (Smooth-On, Dragon Skin 10) and 3D printed molds (Fig. 3). The silicone was poured in the molds at room temperature and left for 12 h to cure. Each arm had a conical shape with the base radius of 30 mm, tip radius of 3 mm, and length of 300 mm. A waterproof servomotor (HS-5086WP, Hitec, USA) was then connected to each arm. These servomotors were arranged on the chain links made with similar spacing distance such that in the octopus-inspired morphology, diametrically opposite arms move in the same plane and in the fish-inspired morphology, arms are aligned side by side (Fig. 2). The chain links were made of 3D printed ABS parts. A carbon rod of 3 mm diameter was used as a shaft for each hinge of chain links. The chain links were connected to the central waterproof servomotor (HS-

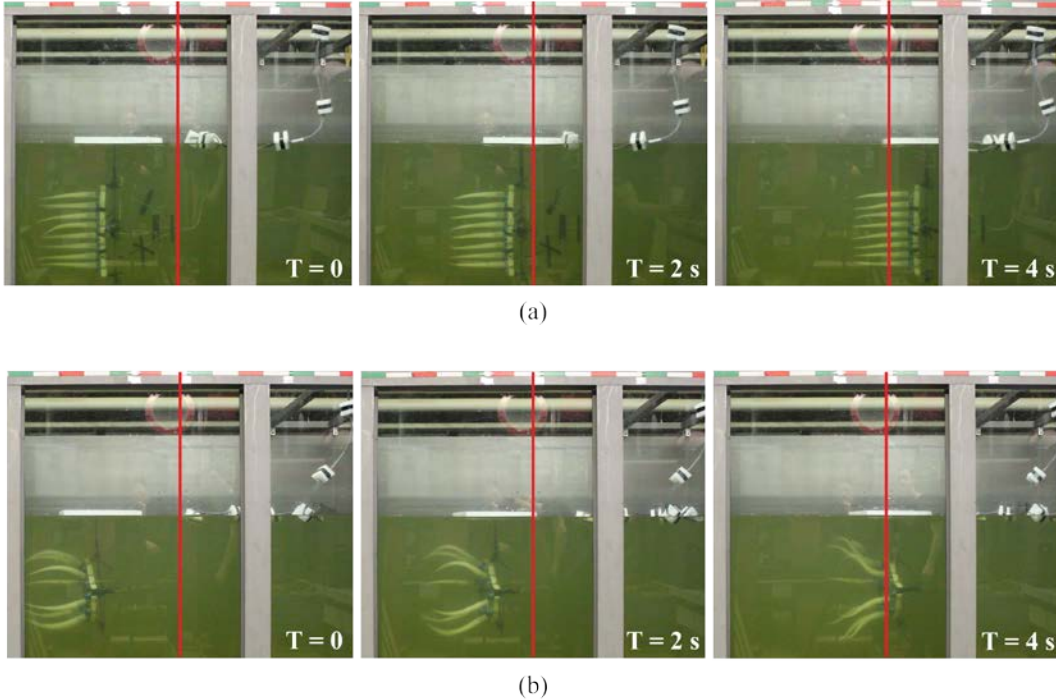


Fig. 4. Forward swimming locomotion of the robot in (a) the fish-mode and in (b) the octopus mode.

5646WP, Hitech, USA) via four 6 mm square carbon rods, 3D printed sliders, and cranks made of a carbon rod of 3mm diameter.

In the octopus-mode, the chain links form a circle of 28 cm diameter. In the fish-mode, the same parts form a 40 cm straight line. A head part (50×25 cm) made of 4 mm thick acrylic plate is attached in front of the robot. The buoyancy of the prototype was adjusted by fixing a foam strip to the chain and a foam plate staying at the surface and keeping the overall robot completely submerged. The overall weight of the prototype was 2.1 kg, and the dimensions were 60 cm long and 50 cm wide.

IV. CHARACTERIZATION OF PROTOTYPE

In this Section, we evaluate the robot in terms of the cost of transport and the swimming efficiency to clarify the effect of adaptive morphology in forward swimming. To assess these characteristics, the swimming speed, thrust force and electrical power consumption were measured.

A. Experimental Set-up

The prototype was tethered and controlled via a micro controller board (Arduino), a computer, and an external power supply (Keithley series 2260B 720W). We recorded the current and voltage from the external power supply to measure the power consumption. The servomotors were driven at a constant voltage of 6V. We performed the experiments inside a water tank ($300 \times 150 \times 150$ cm). In the swimming speed measurement, the position of the prototype was recorded with a camera and a scale (Fig. 4). The speed was obtained by measuring 3 times and taking their average. The thrust force was measured using a load cell (Nano 17, ATI Industrial Automation) and the data was acquired via a computer. The force value was taken by averaging for 5 sec.

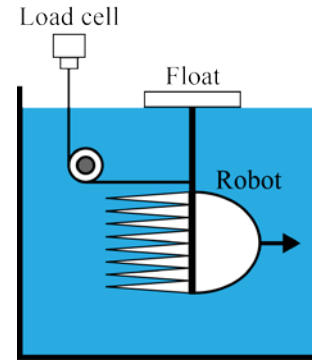


Fig. 5. Thrust force measurement setup.

The setup for the force measurement shown in Fig. 5 is consisted of a 3D printed pulley made of ABS material and a string connected to the load cell. The force value was taken by averaging for 5 sec.

For the driving condition of the octopus-mode, we chose sawtooth waveform with 30° amplitude and 30° offset, which was an optimized value of other octopus robots reported in [8]. On the other hand, the fish-mode was driven with sine waveform with 30° amplitude, which was a common waveform used in many fish robots [11], [12]. With these waveforms, the robot was characterized in the driving frequency range of 0-4 Hz.

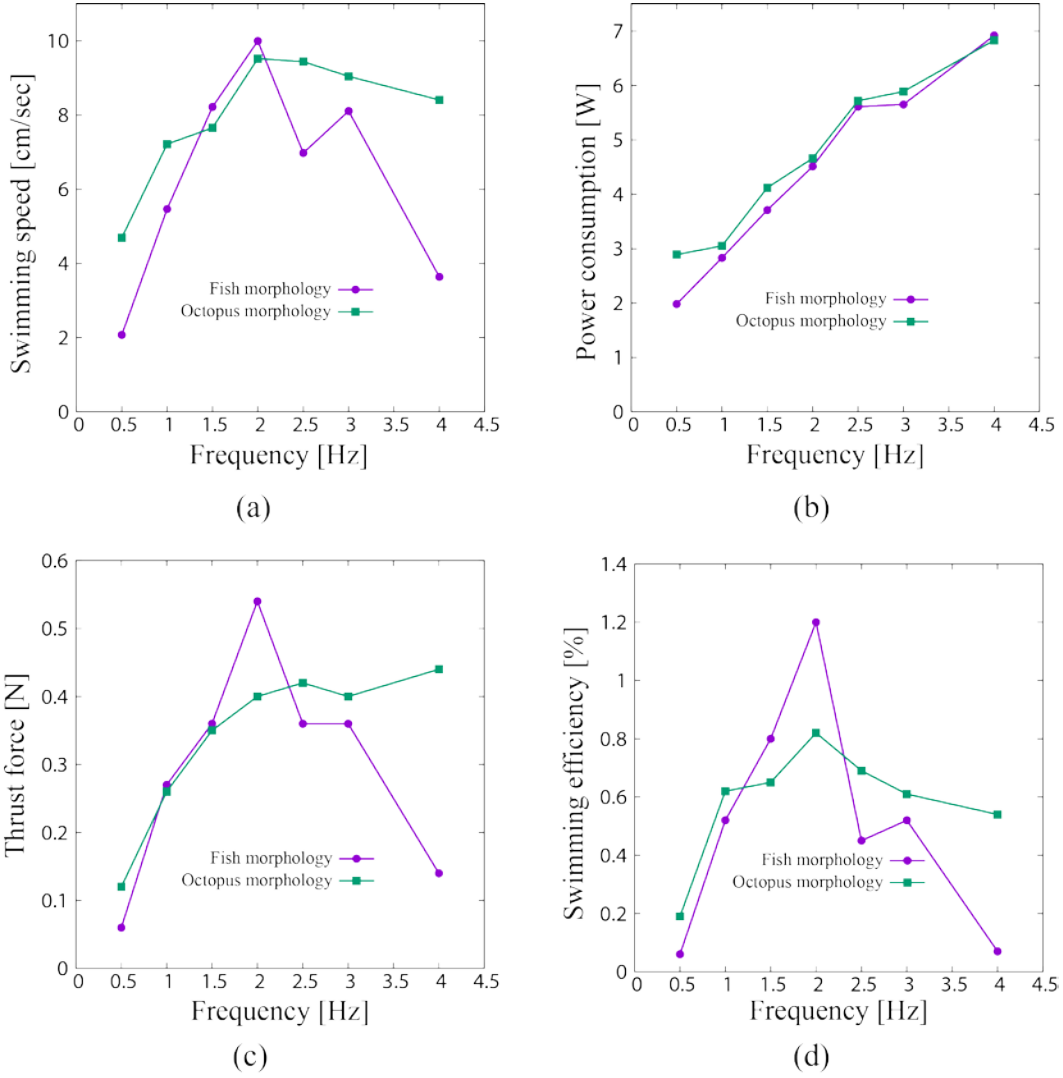


Fig. 6. Results of the characterization of the prototype for the fish and octopus swimming morphologies. (a) Swimming speed as a function of the driving frequency. (b) Power consumption as a function of the driving frequency. (c) Thrust force as a function of the driving frequency. (d) Swimming efficiency as a function of the driving frequency.

B. Result of Swimming Speed, Power Consumptions, and Thrust Force Measurements

Fig. 4(a) and (b) show forward swimming of the prototype in the fish-mode and the octopus-mode, respectively. The robot exhibited a fish-like undulation swimming, and an octopus-like swimming. The measured swimming speed for the fish-mode and the octopus-mode is plotted in Fig. 6(a). The values take a peak at 2 Hz, and the measured speed is 10 cm/s for the fish-mode, and 9.5 cm/s for the octopus mode.

Interestingly, at the frequencies higher than 2 Hz, the reduction of the speed is lower for the octopus-mode. This may have resulted from the difference of the swimming style in the two morphologies. The fish-mode relies on the undulation which could lead to vibration modes in the entire body. On the other hand, in the octopus-mode, the arms are symmetrically oscillated therefore vibration happens only in these parts, leading to different response of the speed on the driving frequency.

Fig. 6(b) shows the power consumptions of the robot as functions of the driving frequency. The trend of the power is similar in the both swimming modes; the power increases with the driving frequency. At 4 Hz, the consumption power was 6.9 W in the fish-mode, and 6.8 W in the octopus mode.

Fig. 6(c) plots the measured thrust force as functions of the driving frequency. Similar to the swimming speed, the forces take a peak at 2 Hz. At this frequency, the average thrust force is 0.54 N in the fish-mode, and 0.40 N in the octopus-mode. In this result, the data shows a trend similar to that of the swimming speed.

C. Swimming Efficiency and Cost of Transport

Based on the results obtained in the previous subsection, we evaluate the robot in terms of the swimming efficiency and the cost of transport. The swimming efficiency of the system is defined by the following equation

$$\eta = \frac{FV}{P_{in}} \quad (1)$$

where, F is the average thrust force, V is the average swimming velocity and P_{in} denotes the average electrical power consumed by the servos driving the arms during a sculling period. Fig. 6(d) is the calculated swimming efficiency using Eq. (1). The efficiency is highest at 2 Hz and takes the value 1.2 % in the fish-mode, and 0.8 % in the octopus-mode.

We then calculate the cost of transport (CoT) at this frequency. CoT of the system is given by the non-dimensional quantity

$$CoT = \frac{P_{in}}{Vmg} \quad (2)$$

where, P_{in} denotes the average electrical power consumed by the servos driving the arms during a sculling period, m is the mass of the robot, and g is the acceleration of gravity. The calculated values of CoT were 2.2 and 2.4, in the fish-mode and the octopus-mode, respectively. These values are close to that of an octopus robot in literature (1.42 [8]).

V. DISCUSSION

The present study addresses, for the first time, development a novel bio-inspired underwater robot with adaptive morphology capable of both fish-like and octopus-like swimming modes. While the octopus-mode was expected to perform original tasks such as object manipulation and ground locomotion as demonstrated in literature [9], it was uncertain if the fish-mode had unique advantages. In this context, we evaluated the robot performance in terms of the swimming efficiency and the cost of transport.

During the characterization, the robot in the fish mode showed faster swimming speed (10 cm/s), larger thrust force (0.54 N), higher swimming efficiency (1.2 %), and lower cost of transportation (2.2) compared to those of the octopus-mode. These results demonstrate a piece of the effect of the adaptive morphology in bio-inspired underwater robots. In addition, the cost of transportation in the two morphologies were close to the reported value of an octopus robot [8].

In this study, we focused on characterizing the robot on the forward swimming as a first step. Further investigation should address maneuverability which includes turning rate in roll, pitch, and yaw axes, and holonomic movements such as backward and lateral movements.

For the future generation of the robot, there is significant potential to improve the robot performance. For example, the design of the robot structure could be modified to align the compliant arms more closely for improving hydrodynamic performance. The use of a compliant web placed on the compliant arms is also a promising approach to improve the performance [13].

Once these investigations and improvements are done, our adaptive morphology underwater robot could enable a wide range of task for different applications. With a lower cost of transport and a greater swimming efficiency, the fish morphology can realize fast and efficient locomotion to travel distant places. In parallel, the octopus morphology can achieve tasks not achievable by the fish morphology, for example crawling at the bottom of the sea to study marine life ecosystem. Besides, the octopus morphology is also adapted for grasping and manipulating objects for submerged structures inspection purpose.

ACKNOWLEDGMENT

The authors would like to thank Cédric Bron for lending his water tank allowing us to conduct experiments. This work was supported by the Swiss National Centre of Competence in Research (NCCR) Robotics.

REFERENCES

- [1] M. Sfakiotakis, D. M. Lane, and J. B. C. Davies, "Review of fish swimming modes for aquatic locomotion," *IEEE Journal of Oceanic Engineering*, vol. 24, no. 2, pp. 237-251, 1999.
- [2] A. D. Marchese, C. D. Onal, and D. Rus, "Autonomous soft robotic fish capable of escape maneuvers using fluidic elastomer actuators," *Soft Robotics*, vol. 1, no. 1, pp. 75-87, 2014.
- [3] K. Suzumori, S. Endo, T. Kanda, "A bending pneumatic rubber actuator realizing soft-bodied manta swimming robot," in *IEEE International Conference on Robotics and Automation*, Roma, Italy, April 2007.
- [4] M. Sfakiotakis, R. Gliva and M. Mountoufaris, "Steering-plane motion control for an underwater robot with a pair of undulatory fin propulsors," in *24th Mediterranean Conference on Control and Automation*, Athens, Greece, June 2016.
- [5] C. Stefanini, S. Orofino, L. Manfredi, S. Mintchev, S. Marrazza, T. Assaf, L. Capantini, E. Sinibaldi, S. Grillner, P. Wallén, and P. Dario, "A novel autonomous, bioinspired swimming robot developed by neuroscientists and bioengineers," *Bioinspir. Biomim.*, vol. 7, no. 2, p. 25001, 2012.
- [6] A. Villanueva, C. Smith and S. Priya, "A biomimetic robotic jellyfish (Robojelly) actuated by shape memory alloy composite actuators," *Bioinspir. Biomim.*, vol. 6, no. 3, p. 036004, 2011.
- [7] S.-W. Yeom and I.-K. Oh, "A biomimetic jellyfish robot based on ionic polymer metal composite actuators," *Smart Mater. Struct.* Vol. 18, no. 8, p. 085002, 2009.
- [8] M. Sfakiotakis, A. Kazakidi and D. P. Tsakiris, "Octopus-inspired multi-arm robotic swimming" *Bioinspir. Biomim.*, vol. 10, no. 3, p. 035005, 2015.
- [9] M. Cianchetti, M. Calisti, M. Margheri, M. Kuba and C. Laschi, "Bioinspired locomotion and grasping in water: the soft eight-arm OCTOPUS robot" *Bioinspir. Biomim.*, vol. 10, no. 3, 2015.
- [10] S. Mintchev and D. Floreano, "Adaptive Morphology: A Design Principle for Multimodal and Multifunctional Robots," *IEEE Robot. Autom. Mag.*, vol. 23, no. 3, pp. 42-54, 2016.
- [11] R. J. Clapham and H. Hu, "iSplash-MICRO: a 50mm robotic fish generating the maximum velocity of real fish," in *IEEE/RSJ International Conference on Intelligent Robots and Systems*, Chicago, IL, USA, September 2014.
- [12] P. V. Alvarado and K. Youcef-Toumi, "Design of machines with compliant bodies for biomimetic locomotion in liquid environments," *Journal of Dynamic Systems, Measurement, and Control*, vol. 128, no. 1, pp. 3-13, 2005.
- [13] M. Sfakiotakis, A. Kazakidi, A. Chatzidaki, T. Evdaimon and D. P. Tsakiris, "Multi-arm Robotic Swimming with Octopus-inspired Compliant Web" *IEEE/RSJ International Conference on Intelligent Robots and Systems*, September 14-18, 2014, Chicago, IL, USA.